

Removal of Solophenyl Red 3BL Dye from Textile Effluents by Adsorption Using a Natural Adsorbent *Oxalis pes-caprae* L.



This work is licensed under a Creative Commons Attribution 4.0 International License

A. Ben Bouabdallah,* F. Mazari, and R. Sifi

Laboratory Food Technology, Faculty of Technology,
Process Engineering Department, M'hamed Bougara
University of Boumerdes 35000, Algeria

doi: <https://doi.org/10.15255/CABEQ.2022.2165>

Original scientific paper
Received: November 27, 2022
Accepted: February 11, 2023

The aim of the present study was to assess the adsorption potential of a natural adsorbent *Oxalis pes-caprae* L. for the removal of azo-dye solophenyl red 3BL (SR 3BL) from textile effluents. The adsorbent was characterized by Fourier transform infrared spectroscopy (FTIR) and scanning electron microscopy (SEM). The effect of various parameters on the efficiency of the adsorption was studied. The optimum was found with the contact time of 35 minutes, pH of 6, and temperature of 25 °C. The equilibrium experimental data were fitted with the Langmuir, Freundlich, and Temkin models. Experimental data were well described with the Langmuir isotherm indicating monolayer adsorption. Pseudo-first-order, pseudo-second-order, and Elovich kinetic models were used to evaluate the adsorption kinetics. The adsorption kinetics was found to follow closely the pseudo-first-order kinetic model. Thermodynamics studies revealed that the adsorption process was spontaneous and exothermic.

Keywords

solophenyl red 3BL, natural adsorbent, *Oxalis pes-caprae*, adsorption kinetics, adsorption isotherms, textile effluents

Introduction

Dyes in water resources cause severe water pollution and block sunlight penetration through water, which impairs photosynthesis of aquatic plants as well as causes a significant alteration in ecological conditions of aquatic life.¹ Dye-contaminated water sources can pose serious public health concerns, including toxicity, mutagenicity, and carcinogenicity among other adverse health effects.²

Dyes are widely used in industries such as textiles, rubber, plastics, printing, leather, cosmetics, etc., to colour their products. As a result, they generate a considerable amount of coloured wastewater.³ Colour removal from wastewater has been a matter of concern, both in the aesthetic sense and health point of view.^{4,5} Colour removal from textile effluents on a continuous industrial scale has been given much attention in the last few years,⁶ not only because of its potential toxicity, but also mainly due to its visibility problem. Many dyes are primarily of synthetic origin and have complex aromatic structures, which make them stable to light, heat and oxidizing agents, and are usually biologically nondegradable.⁷ Hence, they pose a serious threat to human health and water quality, thereby becoming

a matter of vital concern.⁸ Keeping the essentiality of colour removal, concerned industries are required to treat the dye-bearing effluents before releasing them into the water bodies.⁹

The decomposition of dye molecules depends on the complexity of the dye structures.¹⁰ Classified on the basis of their chemical composition and physical properties, they can be acid dyes, azo dyes, basic dyes, disperse dyes, sulphur dyes, pigment dyes, etc.¹¹ About 70 % of dyes used in textile industries are azo dyes with complex structures.¹² Solophenyl red 3BL is an azo dye nonbiodegradable in aerobic conditions and can be reduced to more hazardous intermediate compounds under anaerobic conditions. It is very soluble in water, and its solubility reaches 60 g L⁻¹ at 20 °C.⁷

Several methods are available for the treatment of dyes in water effluents, such as chemical oxidation, flotation, adsorption, electrolysis, chemical coagulation, and biodegradation.¹³ However, adsorption is found to be efficient because of its ease of operation, flexibility, simple design, and ability to treat dyes in a more concentrated form.¹⁴ Some of the advantages of adsorption are possible regeneration at low cost, availability of known process equipment, sludge-free operation and recovery of the adsorbate.¹⁵ The most common adsorbents are zeolites, polymer-based porous materials¹⁶ and activated carbon which is mostly used for its high sur-

*Corresponding author: E-mail: a.ben-bouabdallah@univ-boumerdes.dz

face area. However, its use for dye removal is still very expensive, which is a fact that limits its wide application in the treatment of textile effluents.¹⁷ This has led many researchers to seek more economic and effective adsorbents as potential substitutes for activated carbon,¹⁸ resulting in the interest of adsorbents from biomass to be used as sustainable adsorbents.

Natural plants are applicable for wastewater treatment due to their many advantages and interesting properties.¹⁹ They are abundant, renewable, biodegradable, and inexpensive.^{15,20} It is noteworthy that these plants are undesirable and most of the time they are extracted from nature and discarded or eliminated by chemical processes, which can cause harm to the environment.²¹

The objective of the current research was the removal of solophenyl red 3BL dye from effluents of textile industry using natural plant adsorbent *Oxalis pes-caprae* L. in a powder form (collected from Algerian regions). *Oxalis pes-caprae* L. is a small perennial, herbaceous plant with bulbiferous and underground stem, belonging to family *Oxalidaceae*. Because of its pleasant sour taste, it is also called sourgrass or soursob. High content of oxalic acid is the cause of its sourness.²² This abundant natural plant material may provide an economical and cleaner alternative to replace or supplement present treatment processes for the removal of dyes from textile effluents.

Materials and methods

Reagents

All reagents and chemicals used in this study were of analytical grade. All the solutions were prepared in distilled water.

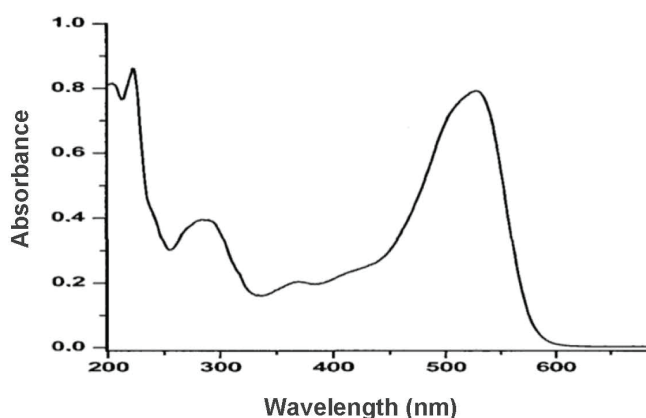


Fig. 1 – Absorption spectrum of SR 3BL

All the acids (H_2SO_4 : sulphuric acid 95–98 %, HCl: hydrochloric acid 32 %, HNO_3 : nitric acid 65 % and H_3PO_4 : phosphoric acid 85 %) were purchased from Sigma-Aldrich.

Sodium hydroxide (NaOH) and sodium chloride (NaCl) were bought from Merck.

Textile dye

Solophenyl red 3BL (SR 3BL) was obtained from the Algerian Textile Company (TEXALG, Algeria). Fig. 1 shows the absorption spectrum of the aqueous solution of SR 3BL (50 mg L^{-1}). The maximum absorption was obtained at the wavelength of 517.6 nm. The molecular structure, molecular weight, and chemical formula of the SR 3BL are shown in Table 1.

Characterization techniques

The absorbance measurements were carried out using a single-beam type UV/visible spectrophotometer (Spectrophotometer Jenway 7315, Boumerdes, Algeria).

Table 1 – Molecular structure, molecular weight and chemical formula of SR 3BL

Chemical dye	Solophenyl Red 3BL
Structure	
Molecular formula	$C_{45}H_{26}N_{10}Na_6O_{21}S_6$
Molecular weight (g mol^{-1})	1373.08

The scanning electron microscopy (SEM) images were obtained using a brand SEM (Philips ESEM XL 30, Tizi-Ouzou, Algeria) equipped with tungsten filament coupled to a complete X-ray microanalysis system.

The Fourier transform infrared (FTIR) spectroscopy was recorded at room temperature between 400 and 4000 cm^{-1} by the standard KBr disk method using (Tracer-100 spectrometer, Boumerdes, Algeria).

Preparation of adsorbent (*Oxalis* powder)

Fresh plant material of *Oxalis pes-caprae* was collected from Algerian regions (Boumerdes) in the flowering stage, washed several times with running water to remove adhering dust and impurities, until clear washing water was obtained, then rinsed with distilled water, and dried at room temperature. After complete drying, the plant was ground to fine powder using an electric grinder (RM 200). The obtained powder was then washed with ethanol to eliminate chlorophyll, was after which it was filtered and oven-dried (Venticell FSNV/5072/16, Boumerdes, Algeria) at 40 °C for 24 hours. Finally, the dried product was placed in a glass bottle, and stored in a desiccator for further use.

Adsorption experimental procedure

The adsorption tests of solophenyl red dye on the natural adsorbent *Oxalis pes-caprae* were conducted in batch mode. In conical flask, undiluted dye effluent (50 mL) was mixed with different masses of the *Oxalis* powder (0.05–0.5 g). The conical flask components were mixed using a magnetic stirrer at 200 rpm until adsorption equilibrium was reached at 35 min. The suspensions were left to settle for 30 min. The contents of the conical flask were filtered, and residual dye concentration γ (mass concentration) in the solution was determined by measuring the filtrate's absorbance at 517.6 nm using a UV-Vis spectrophotometer. Equations (1) and (2) were used to calculate the percentage of removal and the adsorption capacity, respectively:

$$R\% = \frac{(y_0 - y_e)}{y_0} \cdot 100 \quad (1)$$

$$q_e = \frac{(y_0 - y_e)V}{m} \quad (2)$$

where y_0 is the initial dye concentration (mg L^{-1}), y_e is the equilibrium dye concentration (mg L^{-1}), V is the volume of the dye solution (L), m is the mass of adsorbent (g).

In order to find the best operating conditions, the influence of important parameters on the adsorption phenomena was tested: pH of solution (2 to 10), initial temperature of solution (25 to 50 °C), and contact time (5 to 90 min).

Adsorption isotherms

Isotherms are diagrams showing the variation of equilibrium concentration of adsorbent with the liquid phase concentration at a temperature. These models are used to illustrate the adsorbent interaction with the adsorbate, and provide the relationship between the adsorption capacity and the liquid phase concentration of adsorbate under equilibrium conditions at constant temperature.²² The adsorption isotherm analysis was conducted by fitting the adsorption data to Langmuir, Freundlich, and Temkin models.

The Langmuir isotherm,²³ which assumes a surface with homogeneous binding sites, equivalent sorption energies, and no interactions between adsorbed species is expressed by the mathematical relation:

$$q_e = \frac{q_{\max} K_L \gamma_e}{1 + K_L \gamma_e} \quad (3)$$

where q_e is the adsorption capacity at equilibrium (mg g^{-1}), γ_e is the equilibrium dye concentration (mg L^{-1}), q_{\max} (mg g^{-1}) is the maximum adsorption capacity, and K_L is the Langmuir constant (L mg^{-1}).

The Freundlich isotherm,²³ is an empirical model not limited to monolayer coverage alone but also describes multilayer adsorption. The nonlinear form of the Freundlich isotherm is:

$$q_e = K_F \cdot \gamma_e^{1/n} \quad (4)$$

where K_F [$(\text{mg g}^{-1}) (\text{L mg}^{-1})^{1/n}$] and n are Freundlich constants incorporating the factors affecting the adsorption capacity and adsorption intensity, respectively.

The Temkin isotherm²³ assumes linear rather than logarithm decrease in heat of adsorption while ignoring extremely low and very high concentration. It also assumes uniform distribution of bonding energy up to some maximum bonding energy. It is expressed by Eq. (5):

$$q_e = B_T \ln (K_T \gamma_e) \quad (5)$$

where B_T is a constant related to the heat of adsorption and is defined by the expression $B_T = RT/b$, b is the Temkin constant (J mol^{-1}), T is the absolute temperature (K), R is the gas constant ($8.314 \text{ J mol}^{-1} \text{ K}^{-1}$), and K_T is the Temkin isotherm constant (L mg^{-1}).

Adsorption kinetics

An analysis was conducted to determine the adsorption kinetics of dye onto the *Oxalis* powder. The adsorption kinetics for this adsorbent was determined based on the pseudo-first-order, pseudo-second-order, and Elovich models.²⁴ These models were used to analyse the SR 3BL dye removal

process. Eq. (6)²⁴ shows the nonlinear form of the pseudo-first-order model:

$$q_t = q_e(1 - e^{-k_1 t}) \quad (6)$$

where q_e (mg g⁻¹) and q_t (mg g⁻¹) are the amounts of dye removal or adsorbate adsorbed at equilibrium and at time t ; k_1 is the rate constant of this first-order model. The pseudo-second-order equation is written in nonlinear form as follows (Eq. (7)).²⁴

$$q_t = \frac{K_2 q_e^2 t}{1 + K_2 q_e^2 t} \quad (7)$$

where the slope and intercept of (t/q_t) versus t were used to calculate the pseudo-second-order rate constant (K_2) and adsorbate adsorbed at equilibrium (q_e).

The Elovich model isotherm postulates that the adsorption sites increase exponentially with loading, denoting a multilayer adsorption mechanism. The equation of Elovich isotherm²³ is as follows (Eq. (8)):

$$q_t = \frac{1}{\beta} \ln(1 + \alpha \beta t) \quad (8)$$

where q_t and t are as defined above, α is the initial sorption rate (mg g⁻¹ min⁻¹), and β is the desorption constant (g mg⁻¹) during any one experiment.

Thermodynamics study

To calculate the thermodynamic factors that can provide a better understanding of the nature of the adsorption reaction and its feasibility, the Gibbs free energy change (ΔG°), entropy change (ΔS°), and enthalpy change (ΔH°) are required. All of the parameters were calculated at different temperatures, according to Eqs. (9) and (10).²⁴ T (K) is the absolute temperature, K_L is the equilibrium constant, and R (8.314 J mol⁻¹ K⁻¹) is the universal gas constant. The values of ΔH° and ΔS° were calculated based on the slope and y-intercept of Eq. (11)²⁴ for SR 3BL dye.

$$\Delta G^\circ = -RT \ln K_L \quad (9)$$

$$\Delta G^\circ = \Delta H^\circ - T\Delta S^\circ \quad (10)$$

$$\ln K = \frac{\Delta S^\circ}{R} - \frac{\Delta H^\circ}{RT} \quad (11)$$

Desorption and regeneration studies

Desorption studies were conducted to select the optimum desorbing solution to be employed in successive regeneration cycles. Five different desorption agents, 0.1 N NaOH, 0.1 N HCl, 0.1 N NaCl, 0.1 N H₃PO₄, and 0.1 N H₂SO₄, were used to desorb the SR 3BL from the *Oxalis*. Exactly 50 mL of the desorption agents was kept in 100-mL Erlenmeyer flasks with 0.1 g of spent adsorbent, and agitated for 60 min at room temperature. The adsorbate-adsorbent mixtures were filtered after

equilibration using Whatman 42 filter paper. The concentration of SR 3BL dye in the filtrate was determined using a UV-vis spectrophotometer (Spectrophotometer Jenway 7315, Boumerdes, Algeria). Similar protocol was applied but with different HCl acid concentrations (0.05, 0.1, 0.2, 0.3, 0.4, 0.5, and 1.0 M). The regeneration studies were carried out using 0.1 N HCl solution (as it gives optimum desorption elution) for 5 successive cycles of adsorption-desorption. The desorption efficiency was computed using the following equation:

$$\text{Desorption efficiency (\%)} = \frac{C_{\text{des}}}{C_{\text{ads}}} \cdot 100 \quad (12)$$

where, C_{des} is the concentration of SR 3BL dye desorbed in mg g⁻¹, C_{ads} is the concentration of SR 3BL adsorbed in mg g⁻¹.

Results and discussion

Removal of solophenyl red 3BL textile dye

In order to study the removal of SR 3BL by adsorption over the *Oxalis* powder, the effects of various parameters on the adsorption efficiency were investigated.

Effect of pH

The pH parameter plays an important role in the surface charge of the adsorbent, the degree of ionization of the dye in solution, and consequently the adsorption process.²⁵

The experimental runs were made for different pH in the range of 2–12, keeping the other factors constant (adsorbent dose 1 g L⁻¹, initial dye concentration 50 mg L⁻¹, contact time 35 min, temperature 25 °C, volume of dye solution 50 mL). The results are shown in Fig. 2(a).

It is obvious from the figure that the adsorption capacity increased with increasing pH, reaching maximum value at pH of 6. Beyond that, the adsorption capacity began to decrease with increasing pH in the basic medium. The varying trend of pH-dependent adsorption capacity is supported by the concepts of the acid dissociation constant (pK_a) of SR 3BL, two pK_{a1} values corresponding to urea function ($pK_{a1} = 3.6$) and naphtol function ($pK_{a2} = 6.8$), the three sulfonate groups are assumed to have negative pK_a ($pK_a = -2.8$). When $pH < pK_a$, the SR 3BL remains neutral in the aqueous solution, but when $pH > pK_a$, the SR 3BL is found in anionic form.²⁶ The highest removal of SR 3BL was registered at $pH = 6$. After that, the adsorption efficiency reduced, since beyond the pK_a values, the SR 3BL becomes anionic and is repelled by the negatively charged *Oxalis* surface, resulting in decreased adsorption.²⁷

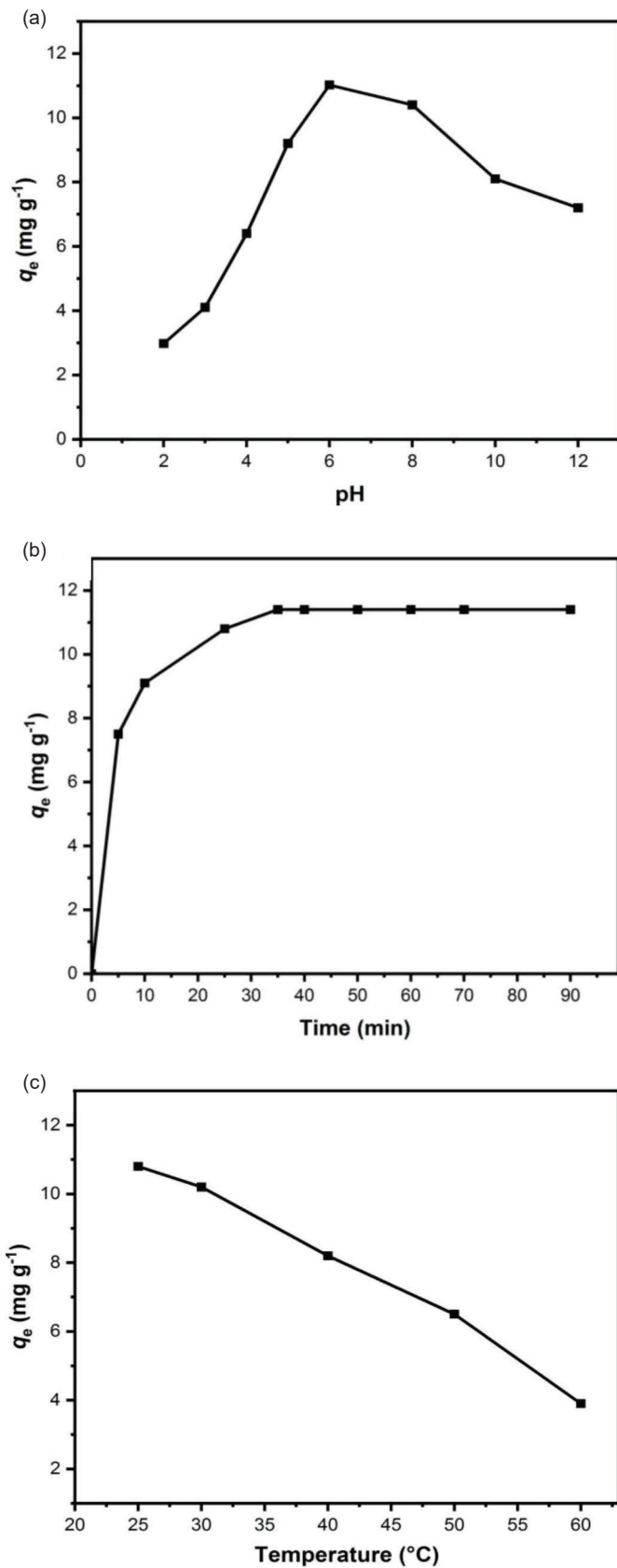


Fig. 2 – Effect of (a) pH; (b) contact time, and (c) temperature on the adsorption of SR 3BL by oxalis (experimental conditions: adsorbent dose 1 g L⁻¹, pH 6, initial dye concentration 50 mg L⁻¹, contact time 35 min, temperature 25 °C, volume of dye solution 50 mL, agitation speed 200 rpm)

Effect of contact time

The effect of contact time is crucial to understand the binding processes of SR 3BL dye and the equilibrium time, which strongly depend on factors like pore structure of adsorbent, adsorbent particle size or surface area, and adsorbent concentration. The contact time was varied from 5 to 90 min, keeping the other factors constant (adsorbent dose 1 g L⁻¹, initial dye concentration 50 mg L⁻¹, pH 6, temperature 25 °C, volume of dye solution 50 mL). The results are shown in Fig. 2(b).

The results showed that the amount of SR 3BL adsorbed on *Oxalis* increased with increasing contact time. It was also observed that the adsorption of SR 3BL was rapid during the first 10 min, and then tended to proceed slowly until about 35 min, where the amount adsorbed was optimal. If the active site on the surface of the adsorbent is saturated by a number of adsorbate particles, the addition of the adsorption time can no longer increase the adsorption capacity.²⁸

Effect of temperature

The effect of temperature is another important physicochemical parameter in explaining the adsorption phenomenon because it modifies the mobility of the pollutant in solution and its adsorption capacity on the adsorbent as well as the thermodynamic process.²⁹ The temperature was varied from 25 to 60 °C, keeping the other factors constant (adsorbent dose 1 g L⁻¹, initial dye concentration 50 mg L⁻¹, pH 6, contact time 35 min, volume of dye solution 50 mL). Fig. 2(c) explains the effect of the temperature on the adsorption of SR 3BL dye by *Oxalis*.

The results showed that the adsorption capacity of *Oxalis* for SR 3BL decreased by increasing the temperature of the dye solution. The decrease in adsorption capacity with increasing temperature indicates that the adsorption is an exothermic process³⁰ and the form of bond between the SR 3BL molecules and the active sites on the surface of *Oxalis* is a physical bond, such that bond breakage occurs at high temperature. The increasing temperature may decrease the adsorptive forces between the dye species and the active sites on the adsorbent surface, which would result in a decreasing adsorption capacity.³¹

Results of the thermodynamics study

The enthalpy (ΔH°) and entropy (ΔS°) parameters were estimated from the classical equations (9) and (10). The plot of $\ln K_L$ versus $1/T$ from equation (11) yielded a straight line (Fig. 3), and the values of ΔH° (kJ mol⁻¹), and ΔS° (J mol⁻¹ K⁻¹) were calcu-

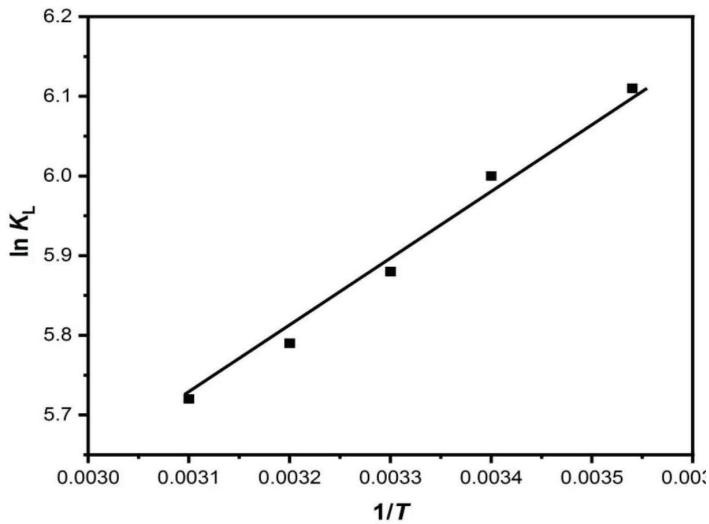


Fig. 3 – Van't Hoff plot of SR 3BL dye adsorption onto Oxalis (experimental conditions: adsorbent dose 1 g L^{-1} , pH 6, initial dye concentration 50 mg L^{-1} , contact time 35 min, temperature $25 \text{ }^\circ\text{C}$, volume of dye solution 50 mL, agitation speed 200 rpm)

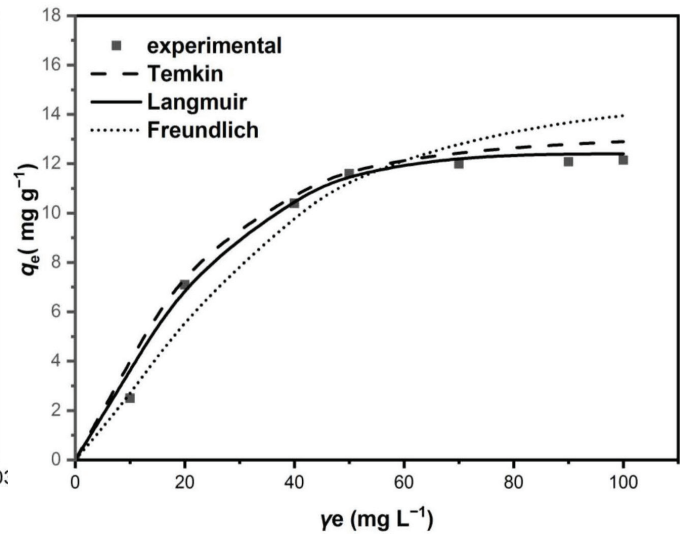


Fig. 4 – Nonlinear fitting of the Langmuir, Freundlich, and Temkin isotherm models for the adsorption of SR 3BL onto Oxalis (experimental conditions: adsorbent dose 1 g L^{-1} , pH 6, initial dye concentration 50 mg L^{-1} , contact time 35 min, temperature $25 \text{ }^\circ\text{C}$, volume of dye solution 50 mL, agitation speed 200 rpm)

Table 2 – Thermodynamic parameters of SR 3BL dye adsorption onto Oxalis

					ΔG° (kJ mol ⁻¹)	ΔH° (kJ mol ⁻¹)	ΔS° (J K ⁻¹ mol ⁻¹)
25 °C	30 °C	40 °C	50 °C	60 °C			
-23.37	-23.58	-23.74	-24.23	-24.39		-35.76	5.68

Table 3 – Adsorption isotherm parameters for SR 3BL dye adsorption onto Oxalis

Adsorbent	Langmuir isotherm			Freundlich isotherm			Temkin isotherm		
	Q_{\max} (mg g ⁻¹)	K_L (L mg ⁻¹)	R^2	K_F (mg g ⁻¹) (L mg ⁻¹) ^{1/n}	n	R^2	B_T	K_T (L mg ⁻¹)	R^2
Oxalis	11.8	2.5	0.998	10.85	2.33	0.952	5.7	4.38	0.987

lated from the intercept and slope of the plots, respectively. The values of ΔG° (kJ mol⁻¹) were calculated from ΔH° and ΔS° (Table 2) using equation (10). The Van't Hoff plot indicates an exothermic adsorption process. The negative ΔG° values confirm the spontaneity of the adsorption process. The positive value of ΔS° suggests the increased randomness at the solid/solution interface during the adsorption process. The exothermic nature of the adsorption was confirmed by the negative value of ΔH° .

Adsorption isotherms

The effect of initial SR 3BL concentration on the adsorption capacity was studied in order to determine the maximum loading capacity of Oxalis. The obtained experimental results were fitted using Langmuir, Freundlich, and Temkin models. Corresponding fits are illustrated in Fig. 4, and the equi-

librium isotherm parameters are listed in Table 3. The values of determination coefficients (R^2) were used in order to evaluate the best-fitted model (Fig. 4). It is clear that the Langmuir and Temkin isotherm models fit the adsorption experiment data better than the Freundlich isotherm model, but the Langmuir isotherm model provides better fitting than Freundlich and Temkin isotherms models by the value of higher correlation coefficient R^2 , which indicates that the adsorption of SR 3BL dye onto Oxalis proceeds by a monolayer formation.

Adsorption kinetics

In order to confirm the experimental data, we utilized the pseudo-first-order, pseudo-second-order, and Elovich models, where kinetic adsorption parameters are shown in Table 4, and the nonlinear plots of three kinetic models are shown in Fig. 5. In

Table 4 – Kinetic parameters of SR 3BL dye adsorption onto *Oxalis*

Pseudo first order			Pseudo second order			Elovich		
q_e (mg g^{-1})	K_1 (min^{-1})	R^2	q_e (mg g^{-1})	K_2 ($\text{g mg}^{-1} \text{min}^{-1}$)	R^2	α ($\text{mg g}^{-1} \text{min}^{-1}$)	β (g mg^{-1})	R^2
11.123	0.072	0.8644	2.602	0.069	0.002	0.523	2.254	0.7748

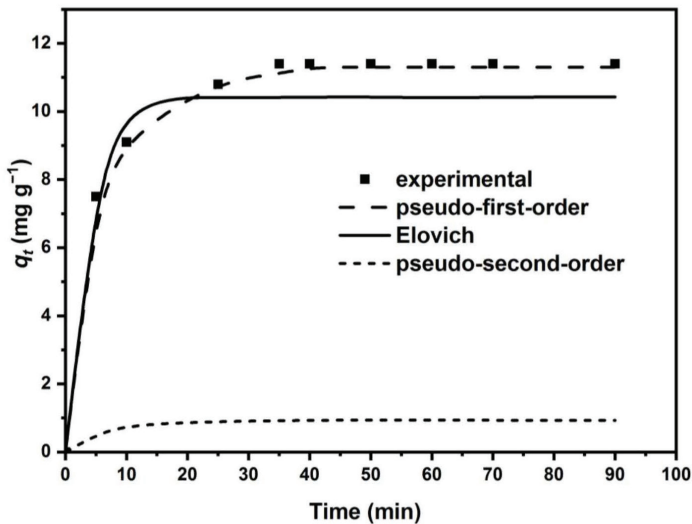


Fig. 5 – Nonlinear plots of pseudo first order, pseudo second order, and Elovich kinetic models for the adsorption of SR 3BL onto *Oxalis* (experimental conditions: adsorbent dose 1 g L^{-1} , pH 6, initial dye concentration 50 mg L^{-1} , contact time 35 min, temperature $25 \text{ }^\circ\text{C}$, volume of dye solution 50 mL , agitation speed 200 rpm)

view of these results, it was observed that the model that best represented the experimental data was the pseudo-first-order, since R^2 is the closest to unity, and the calculated adsorption capacity

($q_e = 11.123 \text{ mg g}^{-1}$) was quite similar to the experimental one ($q_e = 11.8 \text{ mg g}^{-1}$). The pseudo-second-order model cannot be used for description of the experimental data because of the poor R^2 and the low calculated adsorption capacity ($q_e = 2.602 \text{ mg g}^{-1}$) compared to that obtained experimentally.

Characterization of the adsorbent

FTIR analysis

Functional groups have an important role in the process of adsorption of dyes that are influenced by the number of functional groups, types of functional groups, interaction processes, chemical structures, and affinity for adsorbents.²⁸ The results of FTIR analysis of *Oxalis* samples before and after adsorption of SR 3BL are plotted in Fig. 6. The FTIR spectrum of *Oxalis* powder before adsorption of SR 3BL dye (Fig. 6(a)) shows a wide band at 3418.84 cm^{-1} which is due to the OH stretching vibration of the hydroxyl group (OH). A strong peak at 1730 cm^{-1} corresponds to the stretching vibrations of the carboxylic groups of oxalic acid. The intense band at 1050 cm^{-1} is attributed to the O–C–O bond of the oxalate ion (conjugate base of oxalic acid). The adsorption of SR 3BL on the adsorbent may be due to

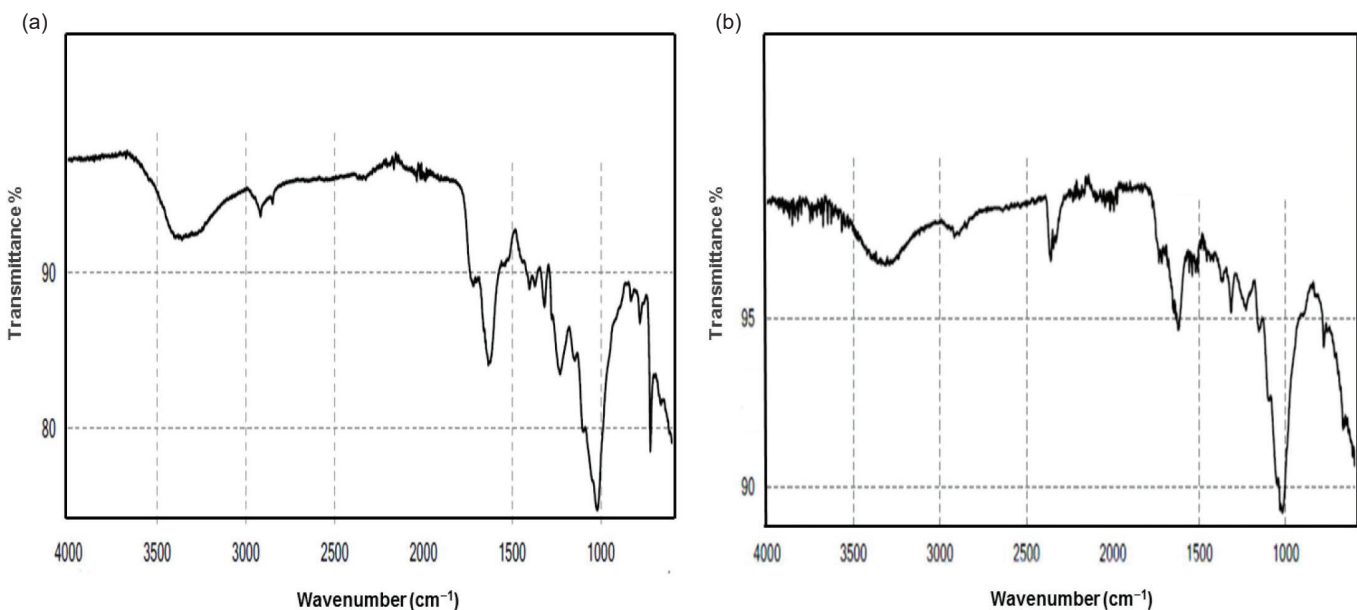


Fig. 6 – FTIR spectrum of *Oxalis* (a) before adsorption of SR 3BL; (b) after adsorption of SR 3BL

the electrostatic attraction between these groups and the cationic dye molecule.³² The FTIR spectrum of *Oxalis* powder after adsorption of SR 3BL dye (Fig. 6(b)) shows characteristic bands associated with *Oxalis* before adsorption, with the appearance of new absorption peaks characteristic of the dye located between 2050 and 2300 cm^{-1} and 2200 and 2300 cm^{-1} corresponding to the vibrations of elongation C=C and C=N, respectively, which confirms the adsorption of SR 3BL by *Oxalis*.

SEM analysis

The scanning electron microscopy images of *Oxalis* powder before and after adsorption of SR 3BL are shown in Fig. 7 with magnification of 1000 \times . The *Oxalis* micrographs before adsorption of SR 3BL (Fig. 7(a)) reveal the presence of many

fine, deep pores, which help greatly to absorb large quantities of SR 3BL molecules on the adsorbent surface. The *Oxalis* micrographs after adsorption of SR 3BL (Fig. 7(b)) indicate that SR 3BL covers the pores and that the pores are no longer visible. This is evidence of SR 3BL adsorption on the adsorbent material surface.

Desorption and regeneration of adsorbent

After the adsorption process is accomplished, the desorption is of great importance to regenerate and reuse used adsorbents, and to reduce the generation of waste as well as keep the process price down.³³ Fig. 8(a) reveals the effects of various chemical agents as eluents on the desorption efficiency. The desorption using 0.1 N HCl was the highest (92.3 %), followed by H_2SO_4 (0.1 N), H_3PO_4

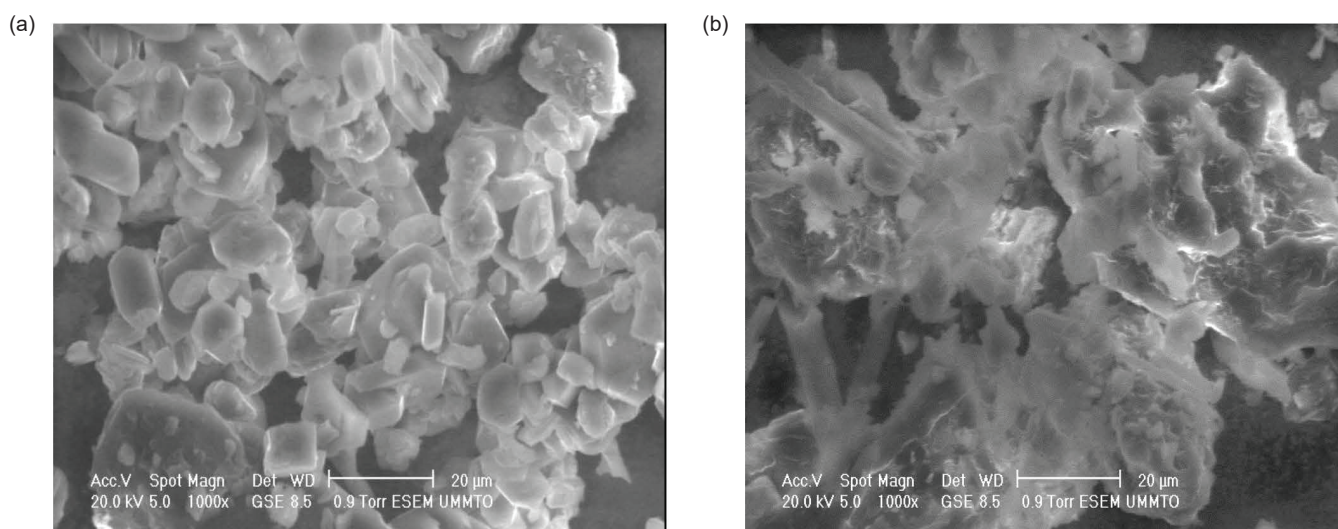


Fig. 7 – SEM images of *Oxalis* (a) before adsorption of SR 3BL; (b) after adsorption of SR 3BL

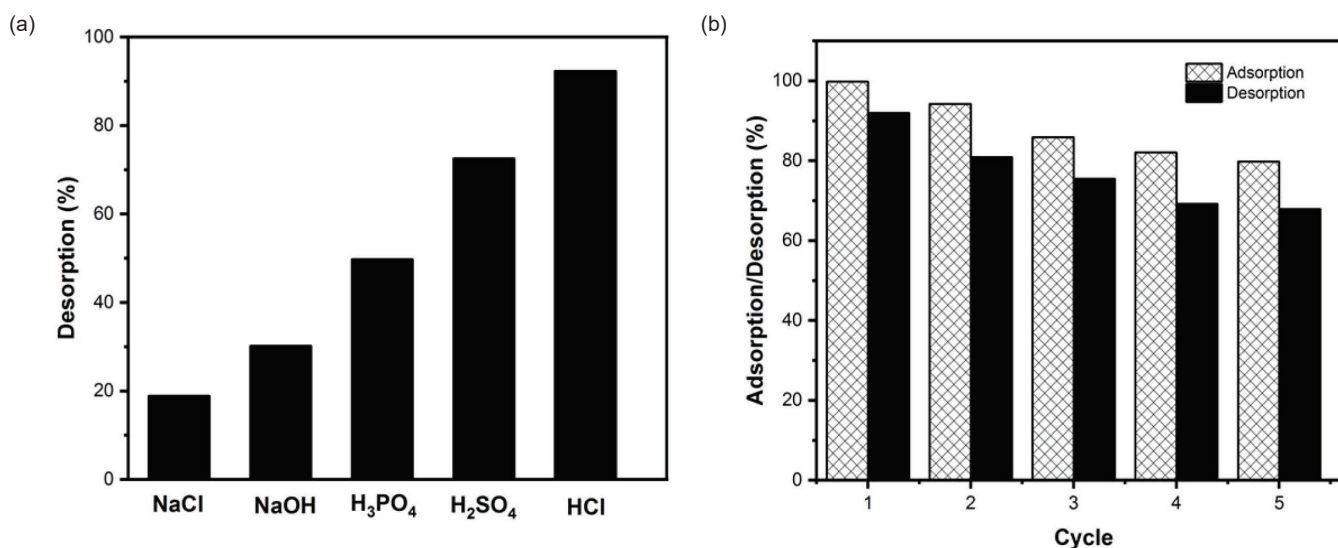


Fig. 8 – (a) Desorption of SR 3BL dye from *Oxalis* using various eluents; (b) adsorption/desorption cycles of SR 3BL dye using HCl (0.1 N) (Adsorption: dosage 1 g L^{-1} , pH 6, contact time 35 min. Desorption: eluent volume 50 mL, dosage 2 g L^{-1} , contact time 60 min. Temperature 25 $^{\circ}\text{C}$)

(0.1 N), NaOH (0.1 N), and NaCl (0.1 N).³⁴ The elution efficiency was further investigated at various HCl concentrations.

The regeneration studies were carried out using a 0.1 N HCl solution (as it gives the maximum desorption) in batch mode for five successive cycles of adsorption-desorption to determine the regeneration efficiency (Fig. 8(b)). The results showed a slight decrease in adsorption for the five cycles carried out, which could be caused by the destruction of certain adsorption sites or functional groups present on the *Oxalis* surface by acid solution.³⁵

Conclusions

A simple and cost-effective treatment procedure was proposed for the removal of SR 3BL from textile industry effluent by adsorption using *Oxalis* plant in its powder form. The experimental conditions for the highest adsorption (11.8 mg g⁻¹) were obtained for an initial concentration of 50 mg L⁻¹ of the dye, a pH of 6, a contact time of 35 min, a temperature of 25 °C, and an *Oxalis* content of 1 g L⁻¹. The characterizations by FTIR and SEM showed the predominance of the physical adsorption mechanism due to the porosity of the material adsorbent and the electrostatic interaction between *Oxalis* and the SR 3BL dye. Modelling study showed that experimental results were well described by the Langmuir isotherm in monolayer adsorption. The reaction kinetics was pseudo-first-order, and the thermodynamic parameters indicated that the nature of the adsorption process was exothermic and spontaneous. This study suggests that adsorption treatment using an abundant and inexpensive natural plant *Oxalis pes-caprae* could be considered as a practical, rapid, and economical alternative for the removal of solophenyl red dye, and more widely, azo dyes.

References

1. Lord, M. D., Neve, G., Keating, M., Budhathoki-Uprety, J., Polycarbodiimide for textile dye removal from contaminated water, *ACS Appl. Polym. Mater.* **4** (2022) 6192. doi: <https://doi.org/10.1021/acsapm.2c00959>
2. Dükkancı, M., Photocatalytic oxidation of rhodamine 6G dye using magnetic TiO₂@Fe₃O₄/FeZSM-5, *Chem. Biochem. Eng. Q.* **35** (2021) 17. doi: <https://doi.org/10.15255/CABEQ.2020.1909>
3. Wang, X., Jiang, J., Gao, W., Reviewing textile wastewater produced by industries: characteristics, environmental impacts, and treatment strategies, *Water Sci. Technol.* **85** (2022) 2076. doi: <https://doi.org/10.2166/wst.2022.088>
4. Lellis, B., Fávoro-Polonio, C. Z., Pamphile, J. A., Polonio, J. C., Effects of textile dyes on health and the environment and bioremediation potential of living organisms, *Biotechnol. Res. Innov.* **2** (2019) 275. doi: <https://doi.org/10.1016/j.biori.2019.09.001>
5. Kumar, U., Vibhute, B., Parikh, S., Experimental study of adsorption efficiency of methylene blue dye by using banana leaf biochar as an adsorbent, *J. Phys.: Conf. Ser.* **1979** (2021) 1. doi: <https://doi.org/10.1088/1742-6596/1979/1/012003>
6. Samsami, S., Mohamadizani, M., Sarrafzadeh, M. H., Rene, E. R., Firoozbahr, M., Recent advances in the treatment of dye-containing wastewater from textile industries: Overview and perspectives, *Process Saf. Environ. Prot.* **143** (2020) 138. doi: <https://doi.org/10.1016/j.psep.2020.05.034>
7. Boutra, B., Trari, M., Nassrallah, N., Bellal, B., Adsorption and photodegradation of solophenyl red 3BL on nanosized ZnFe₂O₄ under solar light, *Theor. Exp. Chem.* **52** (2016) 303. doi: <https://doi.org/10.1007/s11237-016-9482-6>
8. Slama, H. B., Chenari Bouket, A., Pourhassan, Z., Alenezi, F. N., Silini, A., Cherif-Silini, H., Oszako, T., Luptakova, L., Golińska, P., Belbahri, L., Diversity of synthetic dyes from textile industries, discharge impacts and treatment methods, *Appl. Sci.* **11** (2021) 1. doi: <https://doi.org/10.3390/app11146255>
9. Bhatnagar, R., Joshi, H., Mall, I. D., Srivastava, V. C., Electrochemical treatment of acrylic dye-bearing textile wastewater: Optimization of operating parameters, *Desalination Water Treat.* **52** (2014) 111. doi: <https://doi.org/10.1080/19443994.2013.786653>
10. Rane, R., Joshi, S. J., Biodecolorization and biodegradation of dyes: A review, *Open Biotechnol. J.* **15** (2021) 97. doi: <https://doi.org/10.2174/1874070702115010097>
11. Benkhaya, S., El Harfi, S., El Harfi, A., Classifications, properties and applications of textile dyes: A review, *Appl. J. Envir. Eng. Sci.* **3** (2017) 311. doi: <https://doi.org/10.48422/IMIST.PRSM/ajeec-v3i3.9681>
12. Jamee, R., Siddique, R., Biodegradation of synthetic dyes of textile effluent by microorganisms: An environmentally and economically sustainable approach, *Eur. J. Microbiol. Immunol.* **9** (2019) 114. doi: <https://doi.org/10.1556/1886.2019.00018>
13. Vidal, J., Espinoza, C., Contreras, N., Salazar, R., Elimination of industrial textile dye by electrocoagulation using iron electrodes, *J. Chil. Chem. Soc.* **62** (2017) 3519. doi: <https://doi.org/10.4067/S0717-97072017000200019>
14. Slimani, R., El Ouahabi, I., Benkaddour, S., Hiyane, H., Essoufy, M., Achour, Y., El Antri, S., Lazar, S., El Haddad, M., Removal efficiency of textile dyes from aqueous solutions using calcined waste of eggshells as eco-friendly adsorbent: Kinetic and thermodynamic studies, *Chem. Biochem. Eng. Q.* **35** (2021) 43. doi: <https://doi.org/10.15255/CABEQ.2020.1872>
15. Ho, S., Low-cost adsorbents for the removal of phenol/phenolics, pesticides, and dyes from wastewater systems: A review, *Water* **14** (2022) 1. doi: <https://doi.org/10.3390/w14203203>
16. Cui, Y. Y., Zhang, J., Ren, L. L., Cheng, A. L., Gao, E. Q., A functional anionic metal-organic framework for selective adsorption and separation of organic dyes, *Polyhedron* **161** (2019) 71. doi: <https://doi.org/10.1016/j.poly.2018.12.036>
17. Sun, D., Zhang, Z., Wang, M., Wu, Y., Adsorption of reactive dyes on activated carbon developed from *Enteromorpha prolifera*, *J. Anal. Chem.* **4** (2013) 17. doi: <https://doi.org/10.4236/ajac.2013.47A003>
18. Gusmão, G. K. A., Gurgel, A. L. V., Melo, S. T. M., Gil, L. F., Application of succinylated sugarcane bagasse as adsorbent to remove methylene blue and gentian violet from aqueous solutions, Kinetic and equilibrium studies, *Dyes Pigm.* **92** (2012) 967. doi: <https://doi.org/10.1016/j.dyepig.2011.09.005>

19. Boudechiche, N., Mokaddem, H., Sadaoui, Z., Trari, M., Biosorption of cationic dye from aqueous solutions onto lignocellulosic biomass (*Luffa cylindrica*): Characterization, equilibrium, kinetic and thermodynamic studies, *Int. J. Ind. Chem.* **7** (2016) 167.
doi: <https://doi.org/10.1007/s40090-015-0066-4>
20. Alorabi, A. Q., Alharthi, F. A., Azizi, M., Al-Zaqri, N., El-Marghany, A., Abdelshafeek, K. A., Removal of lead(II) from synthetic wastewater by *Lavandula pubescens* Decne biosorbent: Insight into composition–adsorption relationship, *Appl. Sci.* **10** (2020) 7450.
doi: <https://doi.org/10.3390/app10217450>
21. Silva, F., Nascimento, L., Brito, M., Silva, K., Paschoal, W., Fujiyama, R., Biosorption of methylene blue dye using natural biosorbents made from weeds, *Materials* **12** (2019) 1.
doi: <https://doi.org/10.3390/ma12152486>
22. Haque, A. N. M. A., Sultana, N., Sayem, A. S. M., Smriti, S. A., Sustainable adsorbents from plant-derived agricultural wastes for anionic dye removal: A review, *Sustainability* **14** (2022) 1.
doi: <https://doi.org/10.3390/su141711098>
23. Amin, M. T., Alazba, A. A., Shafiq, M., Successful application of eucalyptus *Camdulensis* biochar in the batch adsorption of crystal violet and methylene blue dyes from aqueous solution, *Sustainability* **13** (2021) 1.
doi: <https://doi.org/10.3390/su13073600>
24. Condurache, B. C., Cojocar, C., Samoila, P., Cosmulescu, S. F., Predeanu, G., Enache, A. C., Harabagiu, V., Oxidized biomass and its usage as adsorbent for removal of heavy metal ions from aqueous solutions, *Molecules* **27** (2022) 1.
doi: <https://doi.org/10.3390/molecules27186119>
25. Rossetto, R., Maciel, G. M., de Andrade Arruda Fernandes, I., Modkovski, T. A., Semiao, M. A., Brugnari, T., Haminiuk, C. W. I., Açai seeds as a prospective biosorbent for acid dyes removal, *Chem. Biochem. Eng. Q.* **35** (2021) 407.
doi: <https://doi.org/10.15255/CABEQ.2021.1979>
26. Gul, S., Kanwal, M., Qazi, R. A., Gul, H., Khattak, R., Khan, M. S., Khitab, F., Krauklis, A. E., Efficient removal of methyl red dye by using bark of hopbush, *Water* **14** (2022) 31.
doi: <https://doi.org/10.3390/w14182831>
27. Adane, B., Siraj, K., Meka, N., Kinetic, equilibrium and thermodynamic study of 2-chlorophenol adsorption onto *Ricinus communis* pericarp activated carbon from aqueous solutions, *Green Chem. Lett. Rev.* **8** (2015) 1.
doi: <https://doi.org/10.1080/17518253.2015.1065348>
28. Mahapatra, M. K., Kumar, A., Studies on the adsorption of 2-chlorophenol onto rice straw activated carbon from aqueous solution and its regeneration, *Chem. Biochem. Eng. Q.* **36** (2022) 51.
doi: <https://doi.org/10.15255/CABEQ.2021.2004>
29. Khader, E. H., Mohammed, T. J., Albayati, T. M., Comparative performance between rice husk and granular activated carbon for the removal of azo tartrazine dye from aqueous solution, *Desalination Water Treat.* **229** (2021) 372.
doi: <https://doi.org/10.5004/dwt.2021.27374>
30. Annan, E., Arkorful, G. K., Konadu, D. S., Asimeng, B., Doodoo-Arhin, D., Eglewogbe, M., Synthesis and characterization of hydroxyapatite- (HAP-) clay composites and adsorption studies on methylene blue for water treatment, *J. Chem.* **2021** (2021) 1.
doi: <https://doi.org/10.1155/2021/3833737>
31. Soltani, A., Faramarzi, M., Parsa, S. A. M., A review on adsorbent parameters for removal of dye products from industrial wastewater, *Water Qual. Res. J.* **56** (2021) 181.
doi: <https://doi.org/10.2166/wqrj.2021.023>
32. Chen, K., Du, L., Gao, P., Zheng, J., Liu, Y., Lin, H., Super and selective adsorption of cationic dyes onto carboxylate-modified passion fruit peel biosorbent, *Front. Chem.* **9** (2021) 1.
doi: <https://doi.org/10.3389/fchem.2021.646492>
33. Indah, S., Helard, D., Binuwara, A., Studies on desorption and regeneration of natural pumice for iron removal from aqueous solution, *Water Sci. Technol.* **2017** (2018) 509.
doi: <https://doi.org/10.2166/wst.2018.177>
34. Chaouki, Z., Khalil, F., Ijjaali, M., Valdes, H., Rafqah, S., Sarakha, M., Zaitan, H., Use of combination of coagulation and adsorption process for the landfill leachate treatment from Casablanca city, *Desalination Water Treat.* **83** (2017) 262.
doi: <https://doi.org/10.5004/dwt.2017.20743>
35. Assila, O., Tanji, K., Zouheir, M., Arrahli, A., Nahali, L., Zerrouq, F., Kherbeche, A., Adsorption studies on the removal of textile effluent over two natural eco-friendly adsorbents, *J. Chem.* **2020** (2020) 1.
doi: <https://doi.org/10.1155/2020/6457825>